

Photoluminescence associated with basal stacking faults in c-plane ZnO epitaxial film grown by atomic layer deposition

S. Yang, C. C. Kuo, W.-R. Liu, B. H. Lin, H.-C. Hsu, C.-H. Hsu, and W. F. Hsieh

Citation: [Applied Physics Letters](#) **100**, 101907 (2012); doi: 10.1063/1.3692730

View online: <http://dx.doi.org/10.1063/1.3692730>

View Table of Contents: <http://scitation.aip.org/content/aip/journal/apl/100/10?ver=pdfcov>

Published by the [AIP Publishing](#)

Articles you may be interested in

[On the origin of basal stacking faults in nonpolar wurtzite films epitaxially grown on sapphire substrates](#)

J. Appl. Phys. **112**, 113518 (2012); 10.1063/1.4768686

[Epitaxial growth of thin films and nanodots of ZnO on Si\(111\) by pulsed laser deposition](#)

Appl. Phys. Lett. **100**, 132109 (2012); 10.1063/1.3698470

[Exciton localization on basal stacking faults in a -plane epitaxial lateral overgrown GaN grown by hydride vapor phase epitaxy](#)

J. Appl. Phys. **105**, 043102 (2009); 10.1063/1.3075596

[Dependence of the electrical properties of the ZnO thin films grown by atomic layer epitaxy on the reactant feed sequence](#)

J. Vac. Sci. Technol. A **24**, 1031 (2006); 10.1116/1.2209653

[Layer-by-layer growth of high-optical-quality ZnO film on atomically smooth and lattice relaxed ZnO buffer layer](#)

Appl. Phys. Lett. **83**, 2784 (2003); 10.1063/1.1615834

The advertisement features a dark blue background with white and orange text. At the top left, it reads 'NEW! Asylum Research MFP-3D Infinity™ AFM' in large white letters, followed by 'Unmatched Performance, Versatility and Support' in orange. On the right, the Oxford Instruments logo is shown with the tagline 'The Business of Science®'. Below the text are several images: a blue textured surface, a brown textured surface, a yellow and red patterned surface, and a photograph of the MFP-3D Infinity AFM instrument. Text boxes describe the instrument's capabilities: 'Stunning high performance', 'Simpler than ever to GetStarted™', 'Comprehensive tools for nanomechanics', and 'Widest range of accessories for materials science and bioscience'.

Photoluminescence associated with basal stacking faults in *c*-plane ZnO epitaxial film grown by atomic layer deposition

S. Yang,¹ C. C. Kuo,¹ W.-R. Liu,² B. H. Lin,^{1,2} H.-C. Hsu,³ C.-H. Hsu,^{1,2,a)} and W. F. Hsieh^{1,a)}

¹Department of Photonics and Institute of Electro-Optical Engineering, National Chiao Tung University, Hsinchu 30010, Taiwan

²Scientific Research Division, National Synchrotron Radiation Research Center, Hsinchu 30076, Taiwan

³Institute of Electro-Optical Science and Engineering and Advanced Optoelectronic Technology Center, National Cheng Kung University, Tainan 70101, Taiwan

(Received 21 January 2012; accepted 20 February 2012; published online 8 March 2012)

Basal plane stacking faults (BSFs) with density of $\sim 1 \times 10^6 \text{ cm}^{-1}$ are identified as the dominant defect in the annealed ZnO thin films grown on *c*-plane sapphire by atomic layer deposition. The dominant peak centered at 3.321 eV in low-temperature photoluminescence measurements is attributed to the emission from the BSFs. The emission mechanism is considered to be the confined indirect excitons in the region of quantum-well-like structure formed by the BSFs. The observed energy shift of 19 meV with respect to the BSF-bounded exciton at low temperature may be caused by the localization effect associated with the coupling between BSF quantum wells. © 2012 American Institute of Physics. [<http://dx.doi.org/10.1063/1.3692730>]

ZnO, a wide direct band gap material, has attracted much attention for its applications in ultraviolet photonic devices of which the performance is strongly influenced by the structural defects such as impurities, dislocations, and stacking faults. Photoluminescence (PL) has been widely used to study the influence of the defects on the optical properties of ZnO epitaxial films. Many defects associated emissions, including donor bound exciton (D^0X), acceptor bound exciton (A^0X), donor acceptor pairs (DAPs), and emission originated from edge dislocations have been identified.^{1–6} Various deposition methods, such as metal-organic chemical vapor deposition,¹ pulsed laser deposition (PLD),^{6–10} and molecular beam epitaxy,^{3,4} have been employed to fabricate high quality ZnO epi-films. Recently, atomic layer deposition (ALD), which possesses the advantages of atomic-level thickness control, high uniformity, and low growth temperature, has also been employed to grow ZnO epitaxial films.^{11–15} In our previous work,¹¹ *c*-plane ZnO films grown at 200 °C by ALD on *c*-plane sapphire exhibited a non-twisted in-plane orientation, i.e., $\{11\bar{2}0\}_{\text{ZnO}} \parallel \{11\bar{2}0\}_{\text{sapphire}}$, with a large lattice mismatch of $\sim 31.8\%$.⁷ Basal-plane stacking faults (BSF) are identified as the dominant defects in the ALD-grown *c*-plane ZnO layers by transmission electron microscopy (TEM) analysis. Its density ($\sim 1.0 \times 10^6 \text{ cm}^{-1}$) is comparable to what observed in many non-polar ZnO epi-films and significantly higher than what is typically found in PLD-grown *c*-plane ZnO films.^{16–18} BSFs in the materials of wurtzite structure, such as GaN and ZnO, can be considered as a sheet of zinc blend structure embedded in the wurtzite structure and is expected to strongly affect the PL spectrum.^{17–21} However, the exact influence of the BSFs to ZnO luminescence and the associated emission mechanism have rarely been reported. In this work, we performed power-dependent PL at 10 K and temperature-dependent PL

on the annealed *c*-plane ZnO films deposited by ALD on *c*-plane sapphire to examine the nature of the BSF emissions.

The *c*-plane ZnO epitaxial films were grown on *c*-plane sapphire substrates by ALD. Diethylzinc (DEZn) with chemical formula of $\text{Zn}(\text{C}_2\text{H}_5)_2$ and de-ionized (DI) water of 18 MΩ cm were adopted as the zinc and oxygen precursors, respectively. Each growth cycle consists of precursor exposures and N₂ purge following the sequence of DEZn/N₂/H₂O/N₂ with corresponding duration of 5 s/15 s/5 s/15 s. The substrate temperature was maintained at 200 °C under the vacuum of 1–2 Torr during the deposition. This procedure was repeated 200 cycles, yielding a ZnO layer of 100 unit cells along the growth direction, i.e., about 52 nm thick. The as-deposited samples were then annealed at 800 °C for 1.5 h in pure oxygen gas at 1 atm.

Cross sectional TEM specimens were prepared by focused ion beam (FIB), and the TEM images were taken with a Philips TECNAI-20 field emission gun type TEM. The PL measurements were carried out in a closed cycle cryogenic system using a He-Cd laser at 325 nm as the excitation source. The emission was conducted into a spectrometer (TRIAx 320) equipped with a photo-multiplier tube.

A cross sectional TEM image recorded along the $[\bar{1}2\bar{1}0]_{\text{ZnO}}$ zone axis is shown in Fig. 1(a). The associated selected area electron diffraction (SAED) pattern displayed in Fig. 1(b) confirms the single crystalline of the ZnO thin film. Many lateral lines are observed in the cross-sectional image in Fig. 1(a). These lines are also visible in the dark-field (DF) image with diffraction vector g equal to $(10\bar{1}2)_{\text{ZnO}}$ in Fig. 1(c), but are invisible in the DF image with $g = (0002)_{\text{ZnO}}$ in Fig. 1(d). Based on the extinction rules¹¹ and the visibility of these lateral contrast lines with various diffraction vectors, these lines were identified to be intrinsic type BSF (I_1 or I_2) (Ref. 22) whose density is estimated to be about $1 \times 10^6 \text{ cm}^{-1}$.

To examine the optical properties of the ZnO layers, we performed low temperature (10 K) PL measurements. The PL spectra are illustrated in Fig. 2(a). For comparison, a

^{a)}Authors to whom correspondence should be addressed. Electronic addresses: wfhsieh@mail.nctu.edu.tw and chsu@nsrc.org.tw.

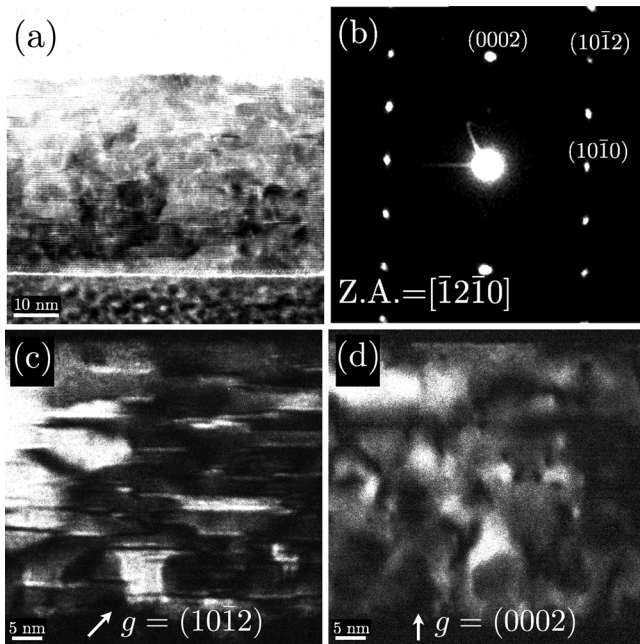


FIG. 1. A cross-section TEM image (a) and a selected area electron diffraction pattern (b) taken along the $[\bar{1}2\bar{1}0]_{\text{ZnO}}$ zone axis of the ALD grown ZnO layer. The dark field images with diffraction vector g set to $(10\bar{1}2)_{\text{ZnO}}$ (c) and $(0002)_{\text{ZnO}}$ (d), respectively.

spectrum taken from a 200 nm thick PLD-grown *c*-plane ZnO film with the BSF density about $4 \times 10^5 \text{ cm}^{-2}$ is plotted in Fig. 2(b). The most intense peak of the PLD-grown sample is the near band edge (NBE) emission originating from D^0X and free-exciton (FX). The other pronounced peaks centered at $\sim 3.330 \text{ eV}$ is attributed to the two-electron satellite (TES) and/or the electrons bound by the stacking faults,²³ and at the lower energy side, a weak peak marked as “FX-1LO” is the typical longitudinal optical phonon replicas of the FX emission.⁸ The two peaks centered at $\sim 3.23 \text{ eV}$ were assigned to DAP and free-electron to acceptor (eA^0) emissions, respectively. In contrast, the spectrum of the ALD grown ZnO shows distinct features. Three peaks, (1) NBE emission at $\sim 3.37 \text{ eV}$, (2) BSF emission at $\sim 3.321 \text{ eV}$,

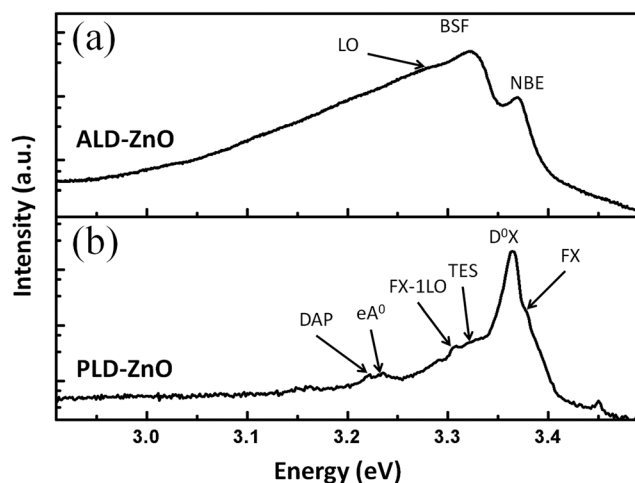


FIG. 2. Low temperature PL spectra taken at 10 K of the ZnO films grown by (a) ALD and (b) PLD methods. The ALD grown ZnO with 50 nm thickness was deposited at 200 °C and annealed at 800 °C in oxygen for 1.5 h. The PLD grown ZnO with 200 nm thickness was deposited on *c*-plane sapphire at growth temperature of 600 °C.

and (3) “LO” emission at 3.28–3.29 eV, were observed. Because the much larger density of BSFs is the dominant difference in structural properties between the ALD- and PLD-grown ZnO films, the observed spectral difference in Fig. 2 may be attributed to the high density of BSFs. To verify this argument, we conducted the following studies.

Figure 3(a) displays the PL spectra of ALD-grown ZnO taken at temperatures between 10 and 280 K. The NBE emission has a rather large line width (FWHM $\sim 22 \text{ meV}$) as compared with those of the PLD-grown ZnO films (FWHM $\sim 10 \text{ meV}$ and typical 9–15 meV).^{7,8} The broad spectra could be caused by defects which reduce the exciton lifetime and thus broaden the FWHM of the exciton transition.¹⁰ Such broadening increases the difficulty to distinguish D^0X from FX emission in the NBE emission. Peak energies of NBE (including both D^0X and FX), BSF, and LO emissions are plotted as a function of temperature in Fig. 3(b). These peak energies decrease monotonically with increasing temperature that can be fitted by the Varshni’s formula, $E(T) = E(0) - aT^2/(T + \Theta_D)$, where $E(0)$ is the energy at $T = 0 \text{ K}$, a is a fitting parameter and Θ_D denotes the Debye temperature, which is set to 920 K according to Refs. 24 and 25. The best fit of the NBE emission energy for temperatures above 100 K, depicted by the dashed curve in Fig. 3(a), yields $E(0) = 3.374 \text{ eV}$ and $a = 1.4 \text{ meV/K}$, which agree well

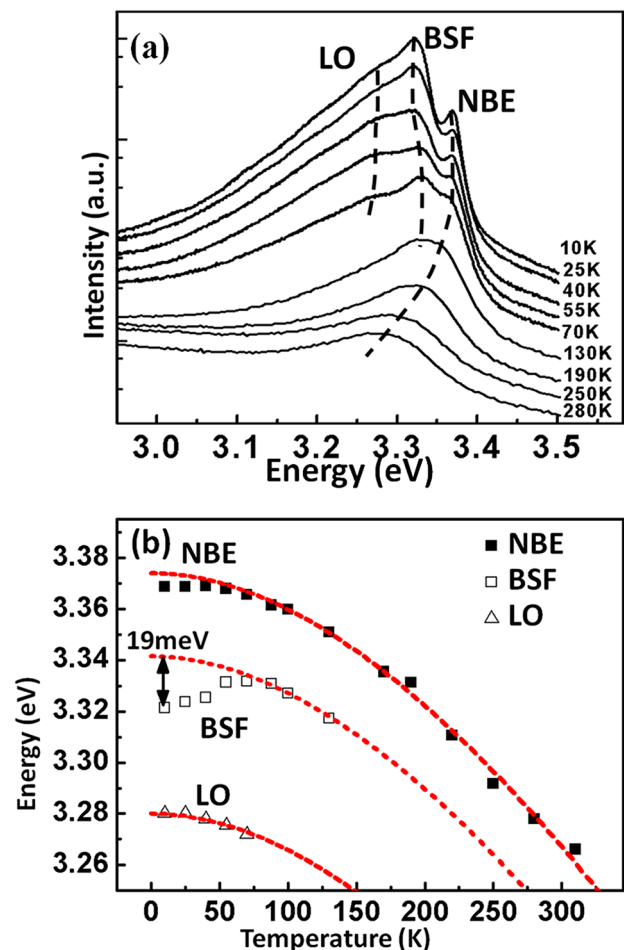


FIG. 3. (Color online) (a) Temperature dependent PL spectra of the ZnO film taken between 10 and 280 K. (b) The energy versus temperature plot of the BSF and NBE emissions. The dashed lines depict the fitting results to the Varshni’s law.

with the FX emission of wurtzite ZnO.^{24–26} The deviation of the experimental data from the fitting curve for temperatures below 100 K is attributed to the contribution of D^0X , which dominates over FX at low temperatures. The weak LO band emission at 3.28–3.29 eV, whose peak position varies complying with the Varshni's formula, is the typical longitudinal optical phonon replicas of the D^0X emission with the phonon energy about 72 meV. The energy of the BSF emission exhibits a different behavior as a function of temperature; it progressively blue shifts from 3.321 to 3.331 eV as the temperature increases from 10 to 88 K and then red shifts with further temperature increase. Fitting the peak energy of the BSF emission above 88 K by the Varshni's formula yields $E(0) = 3.34$ eV, which gives a blue shift of ~ 19 meV with respect to the measured 3.321 eV at 10 K. This phenomenon indicates that the BSF emission could be associated with an exciton transition with energy of 3.34 eV and coupled with a local trap with 19 meV trapping energy.

The emission at ~ 3.321 eV has also been assigned to the DAP transition in ZnO with intentionally doped acceptors, such as N, P, As, and Sb.^{2–5} To clarify the nature of the BSF emission in our ZnO epitaxial films, we performed power dependent PL measurements at 10 K; the spectra are plotted in Fig. 4. The intensities of the NBE and BSF emissions as a function of excitation power P are depicted in the upper-left inset. The peak energy of the BSF emission remains unshifted even though its intensity rises with increasing excitation power. For both the NBE and BSF emissions, their curves of emission intensity versus excitation power nicely follow a power law: $I \propto P^\alpha$ with the exponents $\alpha = 1.31$ and 1.37, respectively. For a free exciton or bound-exciton emissions, the value of the exponent α should fall in the range of $1 \leq \alpha \leq 2$, but for the DAP transitions, α should be less than 1.^{9,27,28} The obtained exponent 1.37 of the BSF emission excludes the mechanism of DAP transition. Together with the absence of peak energy shift with excitation power, the results reasonably infer the BSF emission is associated with excitonic transition.

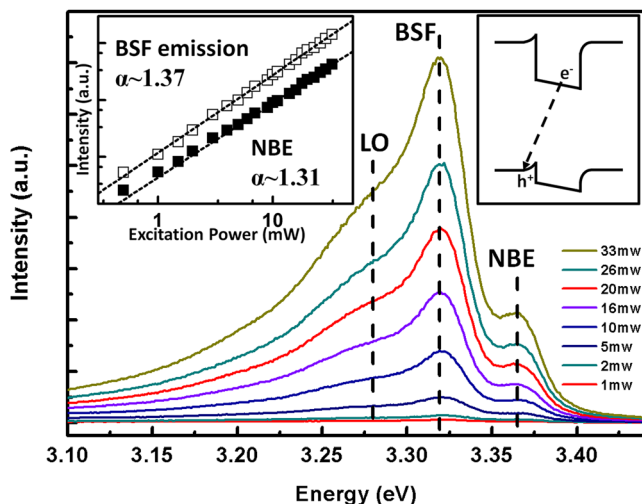


FIG. 4. (Color online) The power dependent PL spectra recorded at 10 K of the ZnO film grown by ALD and annealed at 800 °C. The emission intensity versus the excitation power together with the power law fitting results (dashed lines) of the BSF and NBE emissions are shown in the upper-left inset, and the simple recombination model of the confined indirect excitons in the type-II quantum well is sketched in the upper-right inset.

From the point of atomic stacking sequence, a I_1 and I_2 type BSF in wurtzite structure can be considered as a thin layer of zinc blend structure with a thickness of, respectively, $1.5c$ (0.78 nm) and $2c$ (1.04 nm), where c is the lattice parameter along the c -axis, sandwiched by the wurtzite barriers. According to the *ab initio* calculation,¹⁶ the BSF forms a quantum-well (QW)-like region with negative band offsets in the conduction band minimum (CBM) and the valence band maximum (VBM) with respect to those of the wurtzite barriers. This means that the BSF structure would act as a potential well in the conduction band and a potential barrier in the valence band, and the simple band model is schematized in the upper-right inset of Fig. 4.²¹ Therefore, the obtained $E(0)$ of 3.34 eV by fitting the BSF emission could result from the recombination of the confined indirect excitons in BSF (BSF-EX), which were composed of the electrons captured in the potential wells of the BSF and the holes confined at the interface of BSF and wurtzite structure via attractive Coulomb interaction.²⁹ The 19 meV red shift of the BSF emission from 3.34 eV at temperature about 10 K could be ascribed to the localization effect applied onto the BSF-EX. The localization effect could be attributed to the extrinsic donors (which would bind the BSF-EX) formed by the point defects in or in the vicinity of the QW structures. Moreover, the multiple BSFs could be considered as a coupled QWs structure in which the coupling effect of the electron wave function may be responsible for the localization effect. To consider the reasonableness, the probability density of the electron wave function in single QW (BSF) is estimated about 10% at a penetration length of ~ 3 nm by using a single QW structure with the dimension and potential heights derived from the *ab initio* calculation.¹⁶ As illustrated in Fig. 1, the BSF are distributed in the entire ZnO film with a separation of 2–10 nm along the growth direction (c -axis). They could form coupled QWs structure and lead to the localization effect. Similar phenomenon of the localization of excitons have been reported in the BSF in GaN epi-layers^{17–20} and also observed in the alloy materials such as InGaN,³⁰ AlGaIn,³¹ GaInNAs/GaAs single QW,³² and InGaIn/GaN multiple QWs.³³

High density ($\sim 1.0 \times 10^6$ cm⁻²) of BSF is identified to be the dominant structure defect in the annealed ZnO epitaxial films grown by ALD on c -plane sapphire as verified by TEM and XRD measurements. Each BSF in ZnO is composed of a thin layer of zinc blend structure sandwiched by the wurtzite barriers and forms a type-II QW. The dominant emission centered at ~ 3.321 eV in PL spectra is ascribed to the transition associated with the BSF bounded indirect excitons (~ 3.34 eV) which could be trapped by the local defects and/or the potential induced bundled BSF QWs at low temperatures.

This work is partly supported by National Science Council of Taiwan under Grant Nos. NSC-99-2112-M-006-017-MY3, NSC-100-2112-M-213-002-MY3, and NSC-100-2112-M-006-002-MY3.

¹J. D. Ye, S. L. Gu, F. Li, S. M. Zhu, R. Zhang, Y. Shi, Y. D. Zheng, X. W. Sun, G. Q. Lo, and D. L. Kwong, *Appl. Phys. Lett.* **90**, 152108 (2007).

²Y. R. Ryu, T. S. Lee, and H. W. White, *Appl. Phys. Lett.* **83**, 87 (2003).

³D. C. Look, D. C. Reynolds, C. W. Litton, R. L. Jones, D. B. Eason, and G. Cantwell, *Appl. Phys. Lett.* **81**, 1830 (2002).

- ⁴F. X. Xiu, Z. Yang, L. J. Mandalapu, D. T. Zhao, and J. L. Liu, *Appl. Phys. Lett.* **87**, 252102 (2005).
- ⁵F. X. Xiu, Z. Yang, L. J. Mandalapu, and J. L. Liu, *Appl. Phys. Lett.* **88**, 152116 (2006).
- ⁶W.-R. Liu, Y.-H. Li, W. F. Hsieh, W. C. Lee, M. Hong, J. Kwo, and C.-H. Hsu, *J. Phys. D: Appl. Phys.* **41**, 65105 (2008).
- ⁷W.-R. Liu, W. F. Hsieh, C. H. Hsu, K. S. Liang, and F. S. S. Chien, *J. Appl. Crystallogr.* **40**, 924 (2007).
- ⁸W.-R. Liu, Y.-H. Li, W. F. Hsieh, C.-H. Hsu, W. C. Lee, Y. J. Lee, M. Hong, and J. Kwo, *Cryst. Growth Des.* **9**, 239 (2009).
- ⁹Y. W. Zhang, X. M. Li, W. D. Yu, C. Yang, X. Cao, X. D. Gao, J. F. Kong, W. Z. Shen, J. L. Zhao, and X. W. Sun, *J. Phys. D: Appl. Phys.* **42**, 075410 (2009).
- ¹⁰T. Koida, S. F. Chichibu, A. Uedono, A. Tsukazaki, M. Kawasaki, T. Sota, Y. Segawa, and H. Koinuma, *Appl. Phys. Lett.* **82**, 532 (2003).
- ¹¹S. Yang, B. H. Lin, W.-R. Liu, J.-H. Lin, C.-S. Chang, C.-H. Hsu, and W. F. Hsieh, *Cryst. Growth Des.* **9**, 5184 (2009).
- ¹²C.-S. Ku, H.-Y. Lee, J.-M. Huang, and C.-M. Lin, *Cryst. Growth Des.* **10**, 1460 (2010).
- ¹³L. Dunlop, A. Kursumovic, and J. L. MacManus-Driscoll, *Appl. Phys. Lett.* **93**, 172111 (2008).
- ¹⁴S. J. Lim, S.-J. Kwon, and H. Kim, *Appl. Phys. Lett.* **91**, 183517 (2007).
- ¹⁵P. F. Carcia, R. S. McLean, and M. H. Reilly, *Appl. Phys. Lett.* **88**, 123509 (2006).
- ¹⁶Y. Yan, G. M. Dalpian, M. M. Al-Jassim, and S.-H. Wei, *Phys. Rev. B* **70**, 193206 (2004).
- ¹⁷W. Rieger, R. Dimitrov, D. Brunner, E. Rohrer, O. Ambacher, and M. Stutzmann, *Phys. Rev. B* **54**, 17596 (1996).
- ¹⁸P. Corfdir, P. Lefebvre, J. Levrat, A. Dussaigne, J.-D. Ganière, D. Martin, J. Ristić, T. Zhu, N. Grandjean, and B. Deveaud-Plédran, *J. Appl. Phys.* **105**, 043102 (2009).
- ¹⁹Y. J. Sun, O. Brandt, U. Jahn, T. Y. Liu, A. Trampert, S. Cronenberg, S. Dhar, and K. H. Ploog, *J. Appl. Phys.* **92**, 5714 (2002).
- ²⁰P. P. Paskov, R. Schifano, B. Monemar, T. Paskova, S. Figge, and D. Hommel, *J. Appl. Phys.* **98**, 093519 (2005).
- ²¹A. Konar, T. Fang, N. Sun, and D. Jena, *Appl. Phys. Lett.* **98**, 022109 (2011).
- ²²C. Stampfl and C. G. Van de Walle, *Phys. Rev. B* **57**, R15052 (1998).
- ²³M. Schirra, R. Schneider, A. Reiser, G. M. Prinz, M. Feneberg, J. Biskupek, U. Kaiser, C. E. Krill, K. Thonke, and R. Sauer, *Phys. Rev. B* **77**, 125215 (2008).
- ²⁴V. A. Fonoberov, K. A. Alim, A. A. Balandin, F. Xiu, and J. Liu, *Phys. Rev. B* **73**, 165317 (2006).
- ²⁵D. W. Hamby, D. A. Lucca, M. J. Klopstein, and G. Cantwell, *J. Appl. Phys.* **93**, 3214 (2003).
- ²⁶D. C. Look, D. C. Reynolds, J. R. Sizelove, R. L. Jones, C. W. Litton, G. Cantwell, and W. C. Harsch, *Solid State Commun.* **105**, 399 (1998).
- ²⁷D. Stichtenoth, J. Dürr, C. Ronning, L. Wischmeier, and T. Voss, *J. Appl. Phys.* **103**, 083513 (2008).
- ²⁸T. Schmidt, K. Lischka, and W. Zulehner, *Phys. Rev. B* **45**, 8989 (1992).
- ²⁹Y. T. Rebane, Y. G. Shreter, and M. Albrecht, *Phys. Status Solidi A* **164**, 141 (1997).
- ³⁰Q. Li, S. J. Xu, W. C. Cheng, M. H. Xie, S. Y. Tong, C. M. Che, and H. Yang, *Appl. Phys. Lett.* **79**, 1810 (2001).
- ³¹S. J. Chung, M. Senthil Kumar, H. J. Lee, and E.-K. Suh, *J. Appl. Phys.* **95**, 3565 (2004).
- ³²L. Grenouillet, C. Bru-Chevallier, G. Guillot, P. Gilet, P. Duvaut, C. Vanuffel, A. Million, and A. Chenevas-Paule, *Appl. Phys. Lett.* **76**, 2241 (2000).
- ³³K. S. Ramaiah, Y. K. Su, S. J. Chang, B. Kerr, H. P. Liu, and I. G. Chen, *Appl. Phys. Lett.* **84**, 3307 (2004).